RESEARCH
4(13), January - March, 2018
ISSN 2394–8558
EISSN 2394–8566
Climate Change

Oil Spill Pollution on the Cat Ba Island in northern Vietnam

Doan Quang Tri [1☼], Nguyen Thi Mai Linh [2]

1.Sustainable Management of Natural Resources and Environment Research Group,
Faculty of Environment and Labour Safety,
Ton Duc Thang University,
Ho Chi Minh City,
Vietnam

2.Faculty of Environment and Labour Safety,
Ton Duc Thang University,
Ho Chi Minh City,
Vietnam

☼**Corresponding Author:**
Doan Quang Tri,
Ton Duc Thang University,
Ho Chi Minh City,
Vietnam
Email: doanquangtri@tdt.edu.vn

Article History
Received: 09 October 2017
Accepted: 15 November 2017
Published: January-March 2018

Citation
Doan Quang Tri, Nguyen Thi Mai Linh. Oil Spill Pollution on the Cat Ba Island in northern Vietnam. *Climate Change*, 2018, 4(13), 42-57

ABSTRACT

A 2D oil spill model was applied for the simulation and prediction of oil spill pollution on Cat Ba Island, the northeast Vietnam. The oil spill model has comprised of there modules: Wind-wave module, hydrodynamic module, and spill analysis module in this paper. GIS software was used to establish biological environment surveys and coastal ecosystem maps in the study areas. The results from the wind-wave and hydrodynamic modules showed that the hydrodynamic regime was complicated in the nearshore areas. The results from oil spill model showed that oil spill would affect across a vast area in Cat Ba Island in two scenarios S2 and S3. The oil spill response plan, which is the preparation and sharing providing useful information for ecosystem assessment, habitat conservation, conservation planning and decision-making to minimize damages in case of an oil spill incident.

Keywords: 2D model (HD, SW, SA), GIS software, Oil spill pollution, Cat Ba Island.

1. INTRODUCTION

Industrial growth has been accompanied by imposed environmental risks all around the world (Ajibola and Ladipo, 2011; Kavian et al., 2011; Sekman et al., 2011; Sadatipour et al., 2012; Afandizadeh et al., 2012; Soltani et al., 2012; Rahman and Al-Malack, 2012; Ghasem Zolfaghari et al. 2017; Akbar Mohammadi, 2017). Growing industrialization necessitates the need for oil exploration and transportation, which in turn increases the risks of oil spill accidents. If a spill was to occur today, the "best guess" would probably be a compilation of outputs from different models (Daniel et al., 2002) or even from the same model if using different boundary conditions and data choices. Advanced numerical oil spill modeling can provide emergency response managers with valuable information for risk assessment and contingency planning. Some well-established oil spill models are available to predict oil transport movement and distribution in the water body (Chao et al., 2003). Oil spill movement on water surface has been a significant research focus (Wang et al., 2007), resulting in two-dimensional (2D) oil spill models of advection and spreading (Nagheeby and Kolahdoozan, 2010; Cho et al., 2012; Doan et al., 2013, 2015). The research studies above are some of the foundations for operational oil spill modeling, which focuses on trajectory forecast simulation, probabilistic risk analysis, and information for making real-time responses (William et al., 2013) to minimize impacts and provide a network environmental benefit. Oil spill trajectory models, provide risk assessment, emergency response and contingency planning activities for the surface spills that often result from shipboard accidents and operations, and comprise the majority of oil spills (Deborah et al., 2001).

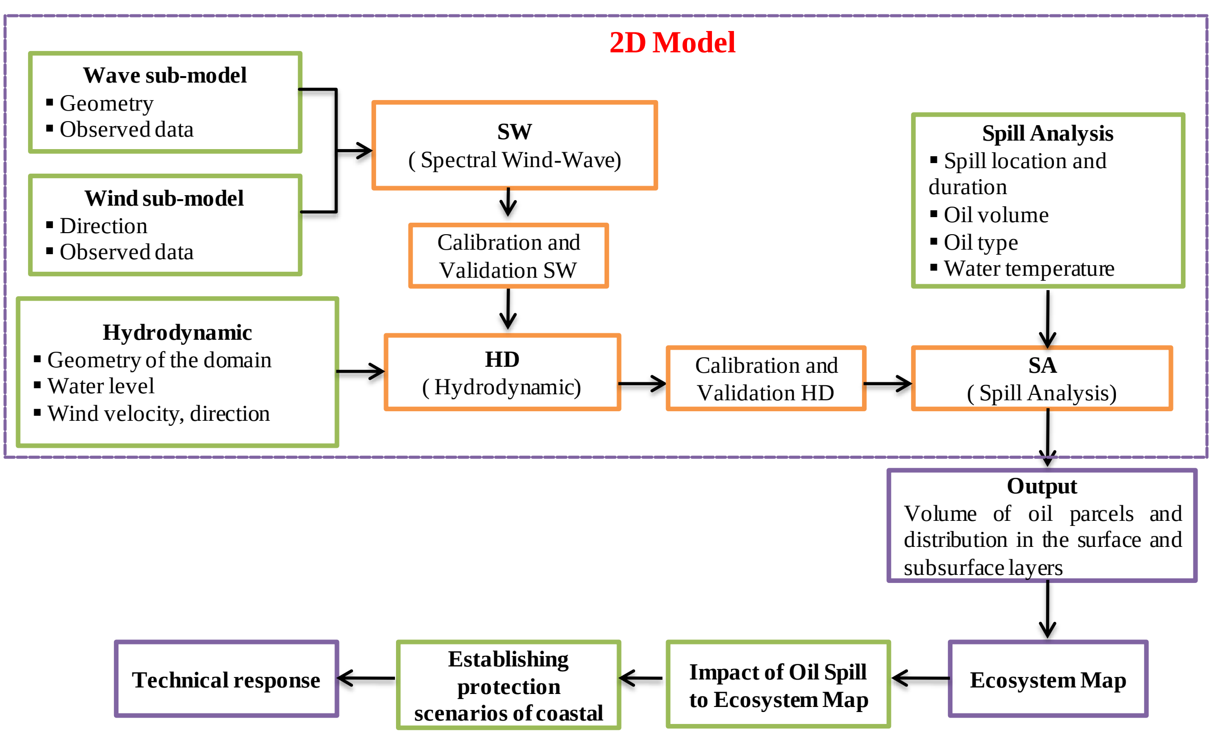

Figure 1 The diagram of the research paper

Most studies investigating the biodiversity of the Cat Ba Islands have concentrated on the characteristics of the major groups of flora and fauna: marine fishes (Quan, 1997), zooplankton (Quan, 1997) and reef-building corals (Yet et al., 2007), mangrove and seagrass beds. The environmental ecosystem maps at Cat Ba Island were established by MapInfo 10.0 software. Spill modeling is an important tool to predict the trajectories and oil fate for devising suitable combating mechanism. This paper represented a two-dimensional simulation model of the oil spill in Lach Huyen Port, Vietnam. The objectives of this study were: (i) To simulate spectral wind-wave (SW) in study site; (ii) to simulate hydrodynamics of the coastal areas; (iii) to simulate oil spill pollution; (iv) to construct impact assessment maps of oil spill on Cat Ba Island and (v) to suggest response plan for oil spill incident. A diagram of the research procedure constructed in Fig. 1.

2. MATERIALS AND METHODS

2.1. Description of study site

Cat Ba is located in the north-east of Vietnam in the northern section of the Tonkin Gulf, and adjacent to Ha Long Bay (the world natural heritage site) (Fig. 2). Cat Ba island has a significant biodiversity value as it is home to a number of rare and endangered species of plants and animals, with the world's rarest primates the Golden-headed langur (FFI, 2003). Biosphere reserves Cat Ba Island has been recognized as a UNESCO World on December 02nd, 2004. It is the 4th world's biosphere reserve in Vietnam. Cat Ba Island has a biosphere reserve of 26,240 ha in acreages; comprised of 17,040 ha of land area and 9,200 ha of sea areas. This paper applies a two-dimensional model to simulate oil spill trajectories of crude oil at different times, which can contribute to remedial observes for actual oil spills.

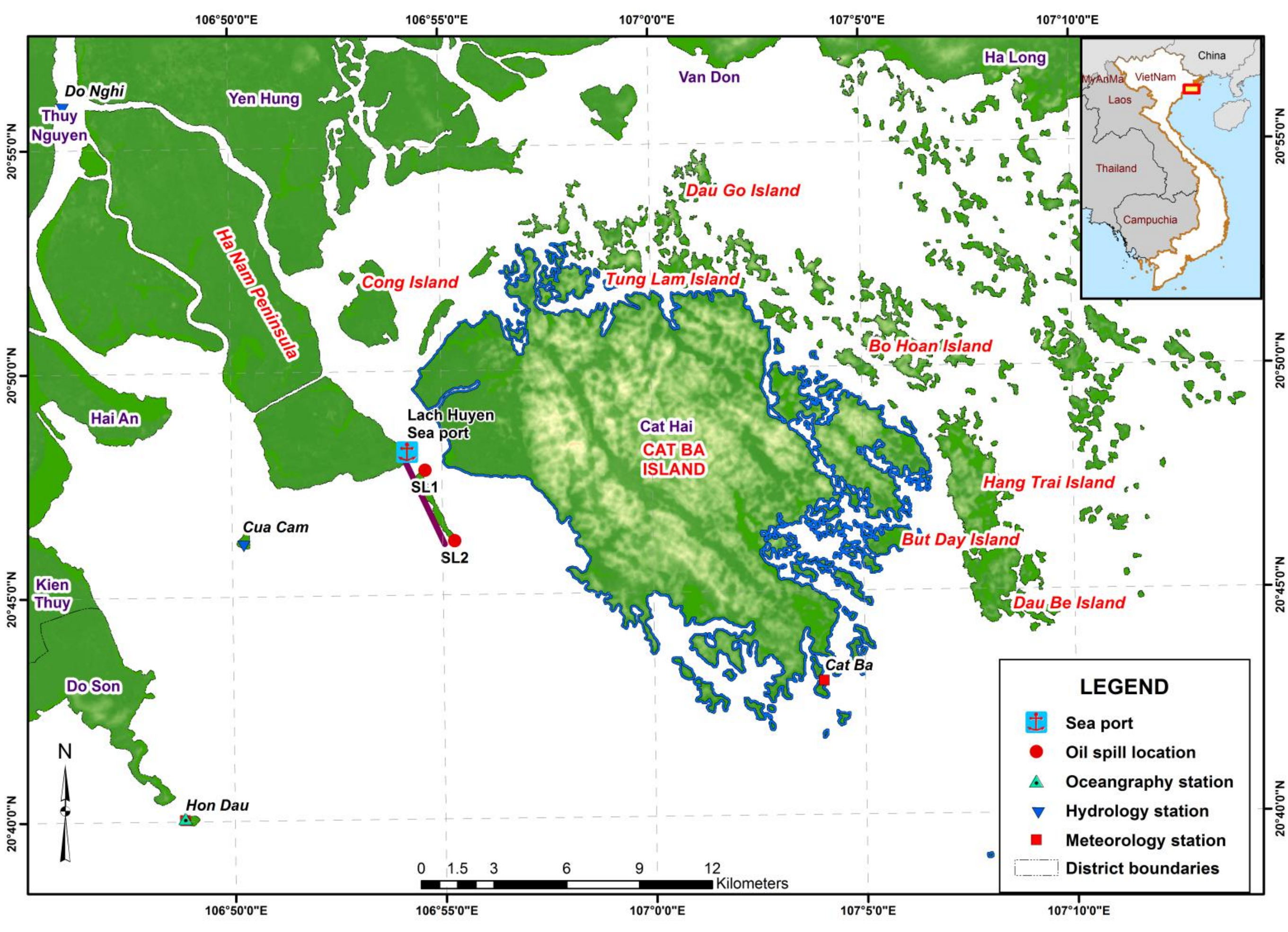

Figure 2 Study location area

2.2. Data collection

2.2.1. Oil spill model

Apart from the storm season lasting from June to November, the wind in the research regions is quite slight. The direction of the wind mainly stretches from east to south according to observable data collected from 1988 to 2015. High wind speeds primarily occurred during the wet season from on March to September. The wind regime in the study area is relatively stable. As the result, we considered the wind data at Bach Long Vi station to be the wind data for the entire area. The waves with the height above 1.0m appear 8.59% and the waves with the direction from East to South appear 60%. However, the high wave has mostly the direction from Southeast to East. The maximum height at Hon Dau station in 20 years from 1965 to 1985 is 5.6m and appears two times. Cat Hai in the Northeast sea of Vietnam affected by 0.92 storms per year. The wave data observed at Hon Dau station in 20 years from 1988 to 2008 are used to calculate the maximum height of wave based on the Gumbel and Weibull distribution method. An average wave data according to the statistical data for Bach Long Vi station from 1988 to 2015 are enlisted in Table 1. Tide data obtained from at Hon Dau oceanographic station. The time periods for the calibration and validation of the spectral wind-wave model were during July 13 - 23, 2013, July 13-23, 2014, respectively. The time period for the calibration and validation of the hydrodynamic model was during July 13 - 23, 2013 and July 13 - 23, 2014, respectively. The period's time simulations for spill analysis model are shown in Table 1.

Table 1 The average speed of wind and wave at Bach Long Vi station

Script	Direction	Wind		Wave		Period time
		Average velocity (m/s)	Frequency (%)	Average wave height (m)	Frequency (%)	
Scenario 1	South East	4.9	8.6%	0.85	7.2%	13 - 23 May 2015
Scenario 2	South	6.7	20%	1.15	17%	13 - 23 July 2015
Scenario 3	South West	5.4	6%	0.8	5%	13 - 23 August 2015

2.2.2. Biological environmental survey

In order to acquire baseline information/data on the biological conditions in and around the Lach Huyen Port project area, field surveys were conducted during May 15-19th (dry season) and August 3-4th (wet season), the field surveys and laboratory analysis were conducted by experts of Institute of Marine Environment and Resources (IMER) under the supervision of HYMETEC. The field surveys covered the following items: Mangrove, Seaweed/seagrass, and Coral. Mangrove, seaweed/seagrass and coral surveys were conducted only in the dry season survey. The location of the field survey sites are shown Fig. 3.

Figure 3 shows the current distribution of the mangrove at the project site based on the analysis of the satellite image Alos avnir-2 in 2010. Most of the mangrove area distribute in the Phu Long commune with the high density. The total area of the mangrove forest is 775.98 ha. However, the mangrove forest can be divided into two parts: outside of the aquaculture ponds (224.74 ha), inside of the aquaculture ponds (551.24 ha). Thus, it is difficult to implement the strategic management plan to revitalize the mangrove forest due to complication in relationship of the public-private partnership.

Table 2 shows the mangrove species identified through the field survey. Eleven species belonging to nine categories were identified. *Rhizophora stylosa* and *Avicennia marina* were the most common species in the survey area. None of the identified species are included in the Vietnam Red Book.

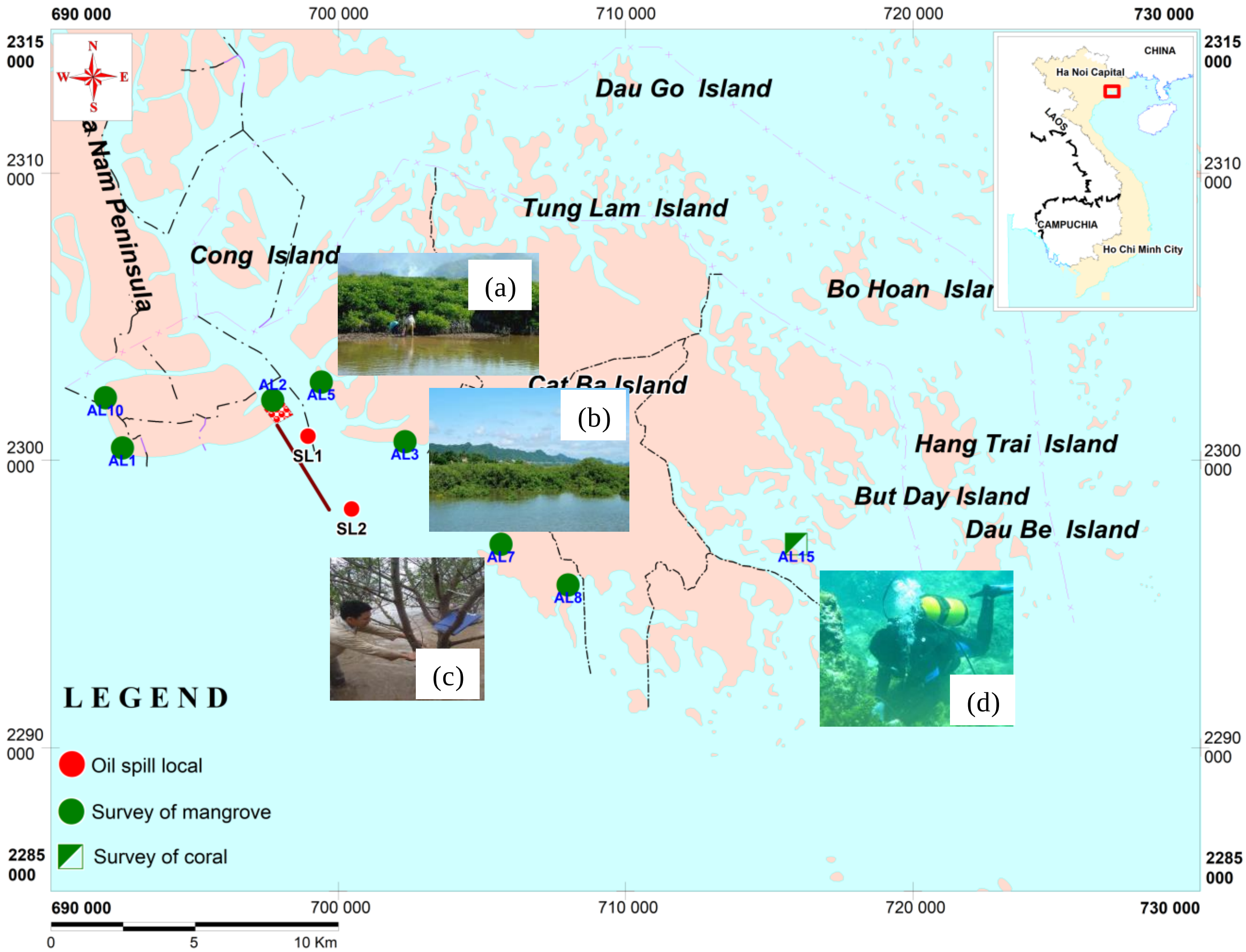

Figure 3 Locations of the field survey sites: Mangrove (a, b, c) and coral (d)

Table 2 List of mangrove species identified through the field survey

No.	Family	Genus/species	Status in Vietnam Red Book	Identified survey sites
1	Sonneratiaceae	*Sonneratia caseolaris*	Not listed	AL10
2		***Rhizophora stylosa***	Not listed	AL1, AL2, AL3, AL5, AL7
3	Rhizophoraceae	*Kandelia obovata*	Not listed	AL5, AL10
4		*Bruguirea gymnorrhiza*	Not listed	AL1, AL3, AL7
5	Aviceniaceae	***Avicennia marina***	Not listed	AL1, AL2, AL3, AL5, AL7
6	Myrsinaceae	*Aegiceras corniculatum*	Not listed	AL1, AL3
7	Pteridaceae	*Acrostichum aureumh*	Not listed	AL10
8	Verbenaceae	*Cleodendrum inerme*	Not listed	AL2, AL10
9	Euphorbiaceae	*Excoecaria agallocha*	Not listed	AL3, AL5
10	Malvaceae	*Hibiscus tiliaceus*	Not listed	AL5

Table 3 shows the hard coral species identified through the field survey. Totally 58 species were identified at the sites AL15 respectively. The diversity of AL15 site was probably lower due to relatively turbid conditions. Within the identified species, 4 species are listed in the Vietnam Red Book namely: Porites lobata, Acropora aspera, Acropora Formosa and Acropora nobilis; which are all classified as "*Vulnerable*". Porites lobata was found at the AL15 site.

Table 3 List of hard coral species identified through the field survey

	Survey site	Family	Genus/species	Status in Vietnam Red Book
1	AL11	Acroporidae	*Acropora pulchra*	Not listed
2		Poritidae	***Porites lobata***	**Vulnerable**
3			*Porites lutea*	Not listed
4			*Goniopora columna*	Not listed
5			*Goniopora lobata*	Not listed
6		Agariciidae	*Pavona decussata*	Not listed
7		Oculinidae	*Galaxea astreata*	Not listed
8			*Galaxea fascicularis*	Not listed
9		Pectiniidae	*Pectinia lactuca*	Not listed
10			*Echinophyllia aspera*	Not listed
11			*Mycedium elephantotus*	Not listed
12		Fungiidae	*Lithophyllon undulatum*	Not listed
13			*Sandalolitha robusta*	Not listed
14		Mussidae	*Lobophyllia hattaii*	Not listed
15			*Lobophyllia hemprichii*	Not listed
16			*Symphyllia. agaricia*	Not listed
17		Merulinidae	*Merulina ampliata*	Not listed
18		Faviidae	*Favia maritime*	Not listed
19			*Favia matthaii*	Not listed
20			*Favia lizardensis*	Not listed
21			*Favia maxima*	Not listed
22			*Favites abdita*	Not listed
23			*Goniastrea pectinata*	Not listed
24			*Goniastrea favulus*	Not listed
25			*Cyphastrea serailia*	Not listed
26			*Echinopora lamellose*	Not listed
27			*Platygyra daelalea*	Not listed
28		Dendrophylliidae	*Turbinaria peltata*	Not listed

MapInfo 10.0 was used as a tool to establish the map. The method used in the construction map is the superposition of the database layers (Fig. 1). The information and background data about the present of the biological environment and around the study scope of Lach Huyen port, the field surveys and laboratory analysis were conducted by experts of the Institute of Marine Environment Resources (IMER) and National Center Hydrometeorological Service (NCHMS). They were measured on May (15-19/5/2015) represents the dry season and on August (3-4/8/2015) represents the rainy season. The results of field survey included as follows: Mangrove forest, seagrass, and shrubs, coral reef, phytoplankton, zooplankton, fish and shrimp, cultivation area, aquaculture pond, hydrographic (Doan and Chen, 2016).

2.3. Model description

In this study, a two-dimensional (2D) MIKE 21 Spill Analysis (SA) was applied to simulate oil spill pollution. A spectral wind-wave (SW) model based on unstructured meshes was applied to simulate the growth, decay and transformation of wind-generated waves, and swells in offshore and coastal areas. The complete spectral formulation is based on the wave action conservation equation (Komen et al., 1994 and Young, 1999). Geographically, an unstructured complex technique is applied. The governing equation in the model is the wave action balance equation, which was formulated in either Cartesian or spherical coordinate. The conservation equation for wave action is expressed as:

$$\frac{\partial N}{\partial t}+\nabla.\left(\bar{v}N\right)=\frac{S}{\sigma} \quad (1)$$

where $N\left(\bar{x},\sigma,\theta,t\right)$ is the action density, t is the time, $\bar{x}=\left(x,y\right)$ is the Cartesian coordinates, $\bar{v}=\left(c_x,c_y,c_\sigma,c_\theta\right)$ is the propagation velocity of a wave group in the four-dimensional phase space $\bar{x},\sigma$ and θ, S is the source term for the energy balance equation and ∇ is the four-dimensional differential operator in the $\bar{x},\sigma,\theta-space$.

$$\sigma=\sqrt{gk\tanh\left(kd\right)}=\omega-\bar{k}.\bar{U} \quad (2)$$

where g is the acceleration of gravity, d is the water depth, $\bar{U}$ is the current velocity vector and $\bar{k}$ is the wave number vector with magnitude k and direction θ .(where g representes the gravity acceleration, d means the depth of water, $\bar{U}$ is the current direct vector and $\bar{k}$ is the number of wave vectors with magnitude k and direction θ .

The governing equations of the HD model are the Saint-Venant equations that are used for two-dimensional space a continuity equation and two momentum equations.

$$\frac{\partial\xi}{\partial t}+\frac{\partial p}{\partial x}+\frac{\partial q}{\partial y}=\frac{\partial d}{\partial t} \quad (3)$$

$$\frac{\partial p}{\partial t}+\frac{\partial}{\partial x}\left(\frac{p^2}{h}\right)+\frac{\partial}{\partial y}\left(\frac{pq}{h}\right)+gh\left(\frac{\partial\xi}{\partial x}\right)+\frac{gp\sqrt{p^2+q^2}}{C^2.h^2}-\frac{1}{\rho_w}\left[\frac{\partial}{\partial x}\left(h\tau_{xx}\right)+\frac{\partial}{\partial y}\left(h\tau_{xy}\right)\right]-\Omega_q-fVV_x+\frac{h}{\rho_w}\frac{\partial}{\partial x}\left(p_a\right)=0 \quad (4)$$

$$\frac{\partial p}{\partial t}+\frac{\partial}{\partial y}\left(\frac{p^2}{h}\right)+\frac{\partial}{\partial x}\left(\frac{pq}{h}\right)+gh\left(\frac{\partial\xi}{\partial y}\right)+\frac{gp\sqrt{p^2+q^2}}{C^2.h^2}-\frac{1}{\rho_w}\left[\frac{\partial}{\partial y}\left(h\tau_{yy}\right)+\frac{\partial}{\partial x}\left(h\tau_{xy}\right)\right]-\Omega_q-fVV_y+\frac{h}{\rho_w}\frac{\partial}{\partial y}\left(p_a\right)=0 \quad (5)$$

where h is the quiet water depth; d is the total depth; ζ is the surface elevation; p, q are the flux velocity in the x and y directions; *C* is the roughness coefficient; g is the gravity vector; f(V) is the wind friction; V, V_x, V_y are the wind velocities and components in the x and y directions; P_a is the air pressure; Ω is the Coriolis parameter; ρ_w is the water density; and τ_{xx}, τ_{yy}, τ_{xy} are the stress components.

The spill analysis model simulates the process of transportation and decomposition, sediment flow or spill in the lake, estuaries, coastal or/and offshore. Pollutants exchange with the surrounding water and are dispersed as a result of random processes in two-dimensions. Oil discharged on a water surface will immediately start to increase its surface area. Mackay et al. (1980b) developed a modified gravity-viscous formulation of Fays theory for area growth. the change of slick area, A_{oil}, with time can be expressed by:

$$\left(\frac{dA_{oil}}{dt}\right) = K_a A_{oil}^{1/3} \left(\frac{V_{oil}}{A_{oil}}\right)^{4/3} \quad (6)$$

where: K_a = constant (s^{-1}); t = time (s); $A_{oil} = \pi R_{oil}^2 (m^2)$; $V_{oil} = \pi R_{oil}^2 . h_s$

The initial oil slick thickness is estimated to be h_s =10cm at t = 0.

Assuming that the actual concentration of hydrocarbons is negligible compared to the solubility, the rate of dissotution is expressed by

$$\frac{dV_{dsi}}{dt} = Ks_i C_i^{sat} X_{moli} \frac{M_i}{\rho_i} A_{oil} \quad (7)$$

where: C_i^{sat} is solubility of fraction i (mg/kg water); X_{mol} is molar fraction of fraction i; M is molar weight of fraction i (kg/mol); ρ is density of fraction i (kg/m^3); A_{oil} is oil slick area (m^2). The mass transfer coefficient for dissolution is calculated by:

$$K_{S_i} = 2.36.10^{-6} e_i \quad (8)$$

where: e_i = 1.4 for alkanes; e_i = 2.2 for aromatics; e_i = 1.8 for oil fines.

3. RESULTS AND DISCUSSION

3.1. Model evaluation statistics

In this paper, NSE, PBIAS and RSR were used to calculate and compare the observed and simulated water levels. With these values, model performance can be judged based on general performance ratings (Table 4). Base on Table 4, model performance can be evaluated as "satisfactory" if NSE > 0.5 and RSR ≤ 0.7 and, for observed data of typical uncertainty, if PBIAS ± 25% for streamflow. The recommended values for adequate model calibration are within the "good" and "very good" performance ratings presented in Table 4.

Table 4 Evaluation criteria for the quality indicators

Performance Rating	RSR	NSE	PBIAS (%)
Very good	0 ≤ RSR ≤ 0.5	0.75 < NSE ≤ 1	PBIAS < ± 10
Good	0.5 ≤ RSR ≤ 0.6	0.65 < NSE ≤ 0.75	±10 ≤ PBIAS < ±15
Satisfactory	0.6 ≤ RSR ≤ 0.7	0.5 < NSE ≤ 0.65	±15 ≤ PBIAS < ±25
Unsatisfactory	RSR > 0.7	NSE ≤ 0.5	PBIAS ≥ ±25

The Nash-Sutcliffe efficiency (NSE) is a normalized statistic that determines the relative magnitude of the residual variance "noise" compared to the measured data variance "information" (Nash and Sutcliffe, 1970). NSE ranges between -∞ and 1.0 (1 inclusive), with NSE = 1 being the optimal value. Percent bias (PBIAS) measures the average tendency of the simulated data to be larger or smaller than their observed counterparts. The optimal value of PBIAS is 0.0, with low-magnitude values indicating accurate model simulation. Positive values indicate model underestimation bias, and negative values indicate model overestimation bias (Gupta et al., 1999). RSR varies from the optimal value of 0, which indicates zero RMSE or residual variation and therefore perfect model simulation, to a large positive value. The lower RSR is, the lower the RMSE, and the better the model simulation performance are. RSR is calculated as the ratio of the RMSE and standard deviation of measured data, as shown in equation 11. NSE and PBIAS are computed as shown in equation 9 and equation 10.

$$NSE = 1 - \frac{\sum_{i=1}^{n}\left(X_i^{sim} - X_i^{obs}\right)^2}{\sum_{i-1}^{n}\left(X_i^{obs} - \overline{X}\right)^2} \quad (9)$$

$$PBIAS = \frac{\sum_{i=1}^{n}\left(X_i^{obs} - X_i^{sim}\right)*100}{\sum_{i=1}^{n}\left(X_i^{obs}\right)} \quad (10)$$

$$RSR = \frac{RMSE}{STDEV_{obs}} = \frac{\sqrt{\sum_{i=1}^{n}\left(X_i^{obs} - X_i^{sim}\right)^2}}{\sqrt{\sum_{i=1}^{n}\left(X_i^{obs} - \overline{X}\right)^2}} \quad (11)$$

where X_i^{sim} is the ith simulated value for the constituent being evaluated; X_i^{obs} is the ith observation for the constituent being evaluated; $\overline{X}$ is the mean of observed data for the constituent being evaluated, and n is the total number of observations.

3.2. Spectral wind-wave model

Topography condition, domain and mesh

The computation domain of the oil spill at Lach Huyen port is covered by unorganized grids (Fig. 4a). The sea route and port berth are geometrically displayed by a computation mesh size of 60m. Accordingly, the mesh size in the offshore areas is mainly developed from unorganized grids method. The detail bathymetry of the hydrodynamic model domain was obtained from the seabed topographic map (Fig. 4b).

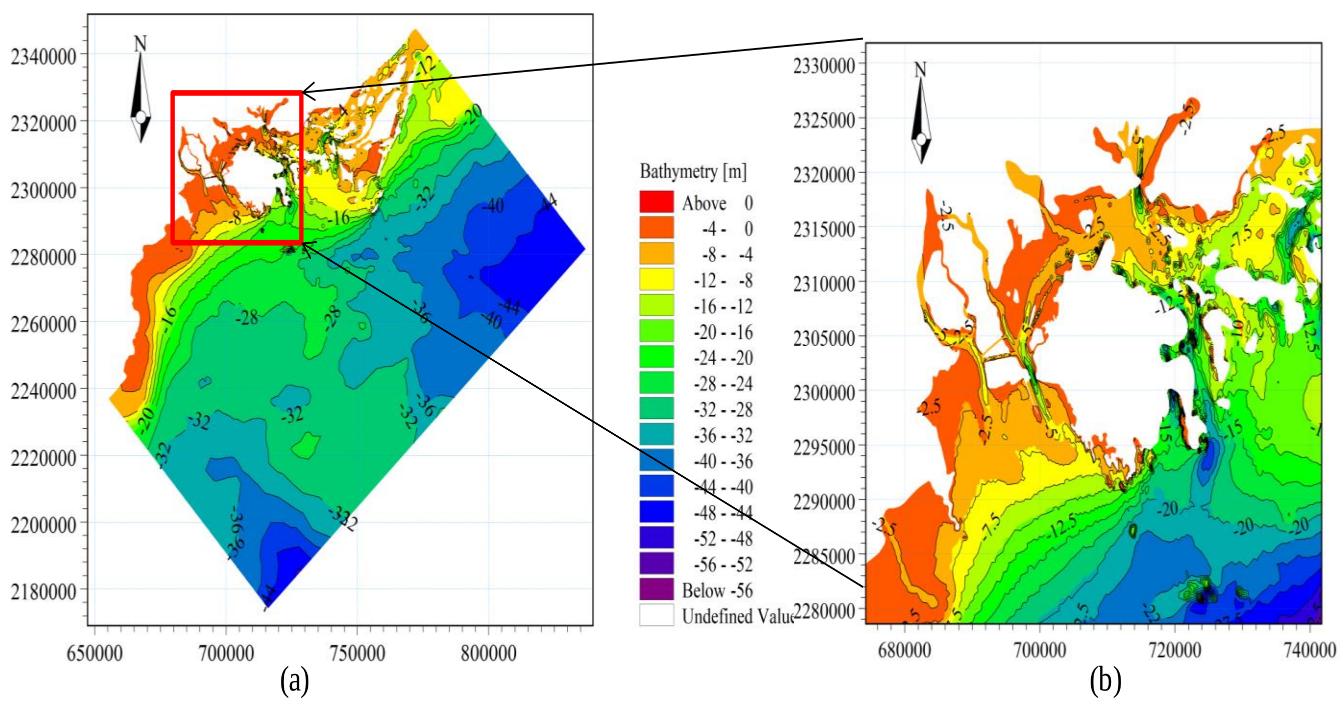

Figure 4. **a**) 2D bathymetry domain and **b**) Detail of bathymetry domain

Calibration and validation of spectral wind-wave model

The calibration and validation of spectral wind-wave is based on the observation of the wave data from July 13-23, 2013 and July 13-23, 2014. The model parameters obtained from the calibration and validation process are as follows: the impact force of the wind is determined by the formula of Karman et al. the wave breaking parameter $\gamma = 0.79$ and the friction parameter $k_N = 0.043$m. Because a wave observing station was not established near the study area, we calculated the wave propagation from the offshore Bach Long Vi marine station. The comparisons of calculated and measured wave height at Hon Dau station showed a satisfactory fit (Figs. 5a, 5c), which is considered a foundation for the calculation of the wave stress filed in given situations. NSE, R^2, RSR, and PBIAS were used to evaluate the quality of the calibration and validation of the spectral wind-wave model (Table 5). NSE values for the calibration and validation ranged from 0.88-0.9. According to the guidelines of model evaluation showed in Table 4, the spectral wind-wave model simulated the streamflow trends very well, as shown by the statistical results which are an agreement with the graphical results. The coefficient of determination (R^2) values ranged from 0.95-0.96 (Figs. 5b, 5d) while the RSR values ranged from 0.31-0.35 for both calibration and validation processing. These results indicate that the model performance for the streamflow regime of residual variation is highly acceptable. The PBIAS values varied from 11.66% to 12.74% for both calibration and validation. An average magnitude of simulated values was within the good performance rating (±10% ≤ PBIAS < ±15%) for both calibration and validation process (Table 4). The impact of the waves can be used to measure the input data fileds of the flow fields in the research sites. Figure 6 displays the computation of wave field from July 14 - 23, 2013.

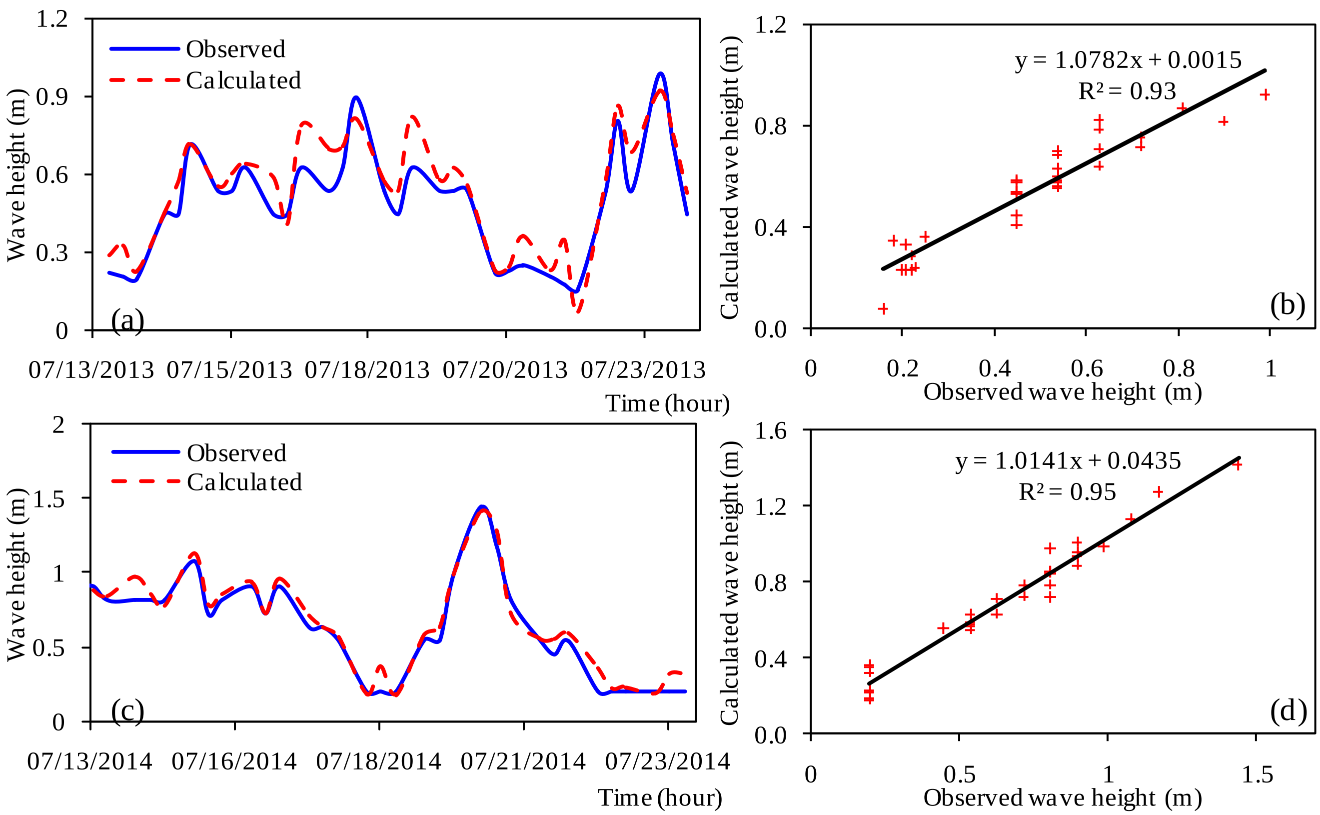

Figure 5. **a**) Calibration of wave height at HonDau from July 13-23, 2013; **b**) Determination coefficient (R^2) between observed and calculated wave height in calibration process; (**c**) Validation of wave height at HonDau from July 13-23, 2014; (**d**) Determination coefficient (R^2) between observed and calculated wave height in validation process

Table 5 The results of calibration and validation spectral wind-wave and hydrodynamic model at Hon Dau station

Processing	Year	Efficiency	Spectral wind-wave	Hydrodynamic
Calibration	2013	R^2	0.95	0.98
		NSE	0.88	0.97

		PBIAS	11.66	-3.02
		RSR	0.35	0.17
Vaidation	2014	R^2	0.96	0.97
		NSE	0.90	0.96
		PBIAS	12.74	-4.02
		RSR	0.31	0.2

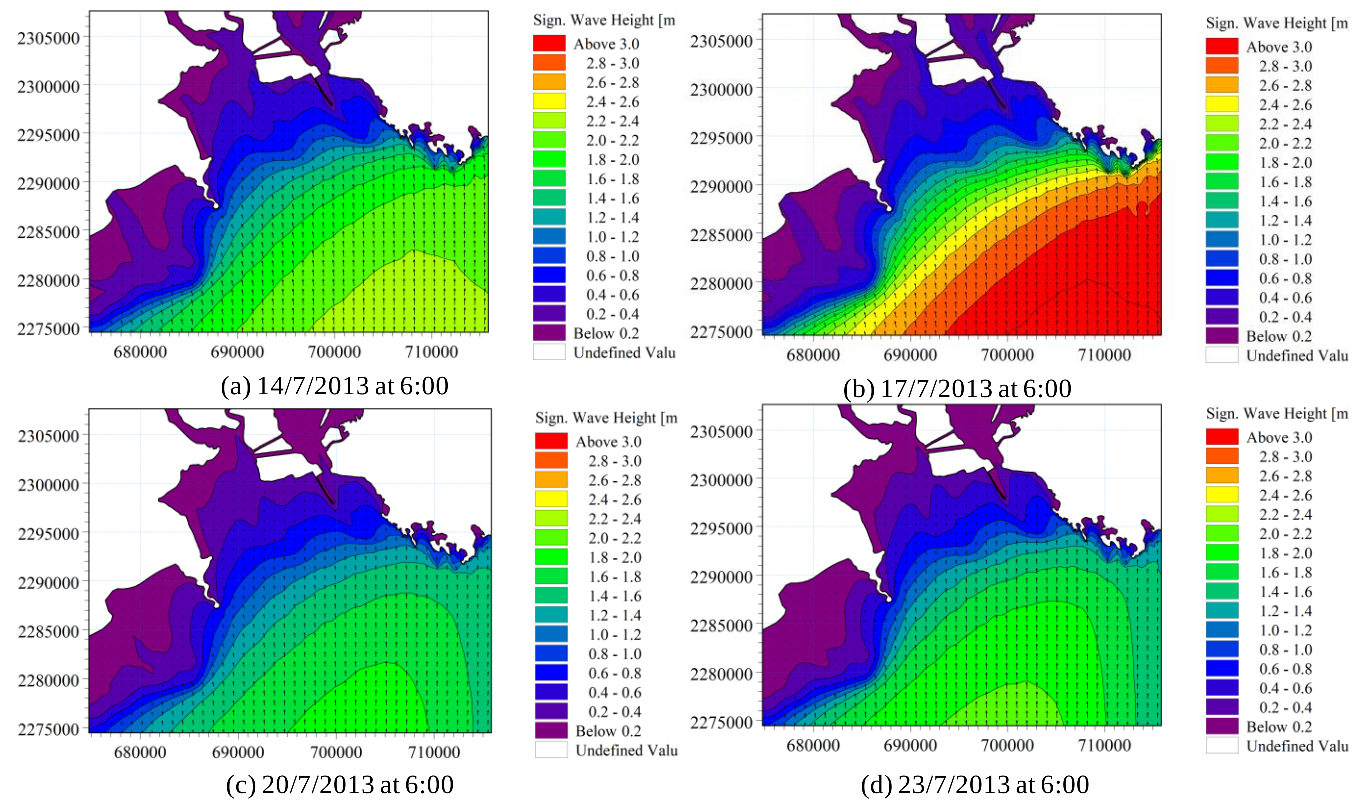

Figure 6 The computed wave field from July 14 to 23, 2013

3.3. Hydrodynamic model

Validation and calibration hydrodynamic model

The 2-D hydrodynamic model is calibrated according to the observed data at Hon Dau marine station during the period of July 13-23, 2013 and July 13-23, 2014, incorporating with the global tidal boundaries with the definition of 0.25 degree and the average wind field. The simulation has been done with the tidal boundary conditions at the downstream of the estuaries. Manning's bed roughness coefficient is the key parameter considered in the calibration. Several trial-and-error runs of the hydrodynamic model were done by varying Manning's roughness coefficient to achieve suitable calibrations between the observed and simulated water levels and streamflow in the study region. The calibration comparison of observed and simulated water level tides in 10 days at Hon Dau station are showed in Fig. 7a. Validation of the model used the observed water levels at Hon Dau marine station during the period of July 13-23, 2014 (Fig. 7c). The results of calculated and observed water levels are in good agreement with vibration amplitude, absolute value, and the tidal phases during both calibration and validation processes (Figs. 7a, 7c). NSE, R^2, RSR, and PBIAS were used to evaluate the quality of the calibration and validation of the model (Table 5). NSE values for the calibration and validation ranged from 0.96-0.97. According to the guidelines of model evaluation showed in Table 4, the 2-D model simulated the streamflow trends very well, as shown by the statistical results which are an agreement with the graphical results. The coefficient of determination (R^2) values ranged from 0.97-0.98 (Figs. 7b, 7d) while the RSR values ranged from 0.17-0.2 for both calibration and validation. These results indicate that the model performance for the streamflow regime of residual variation is highly acceptable.

The PBIAS values varied from -4.02% to -3.02% for both calibration and validation. The average magnitude of simulated values was within the good performance rating (PBIAS < ± 10%) for both calibration and validation. The parameters in the calibration process are used in the model validation with varying Manning's roughness coefficient from 28-32 ($m^{1/3}/s$). An appropriate pattern was achieved; the parameters of it can act as a validation and an oil spill model. The outcomes of the oil spill simulation described in the next section are considerably affected by the combination of wave regime and wind as well as strong tidal changes. The outcomes of the validation and calibration demonstrated the suited simulation of hydrodynamic process. The model therefore can be applied to measure the oil migration.

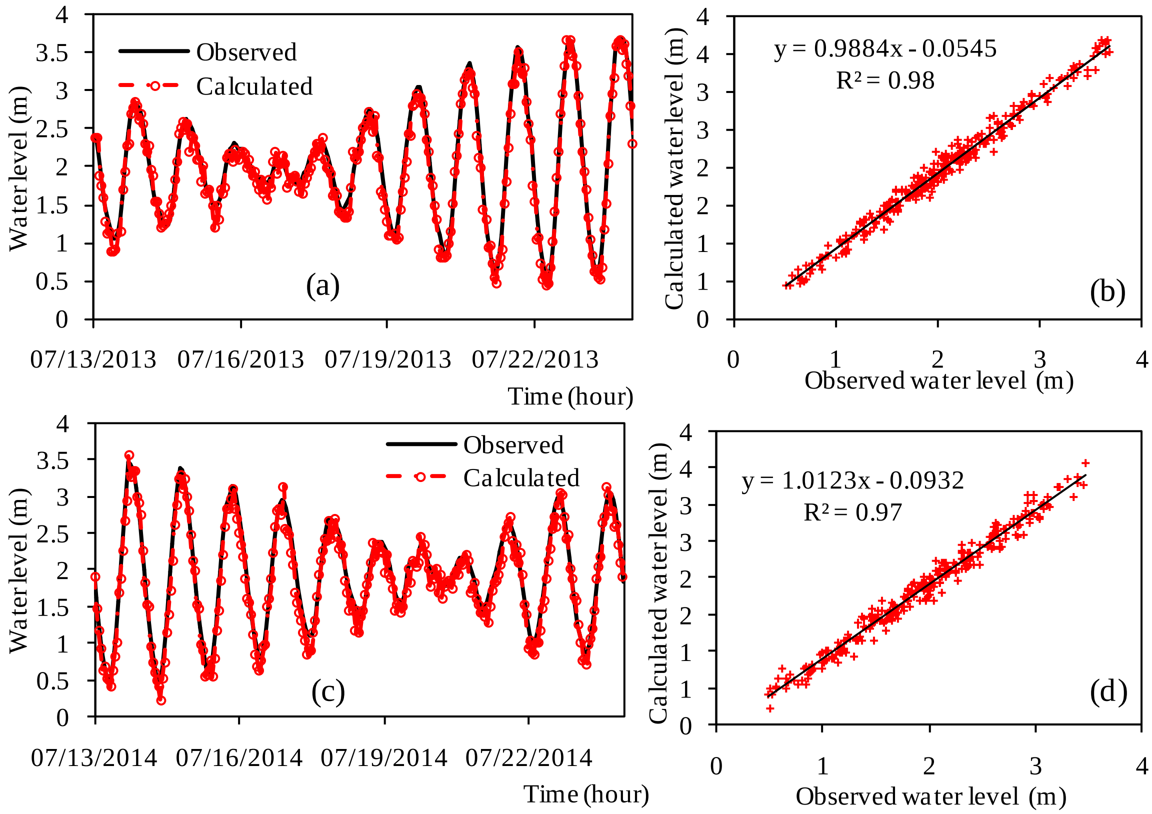

Figure 7. **a**) Calibration of water level at Hon Dau from July 13-23, 2013; **b**) Determination coefficient (R^2) between observed and calculated wave height in calibration process; (**c**) Validation of water level at Hon Dau from July 13-23, 2014; (**d**) Determination coefficient (R^2) between observed and calculated wave height in validation process.

3.4. Spill analysis model

Out of the research data, 2000 tons of oil overflow in 10 successive days were supposed in location SL1 or location SL2; where SL1 is located at the head of the creek with UTM-48 coordinates (700095, 2298279) and SL2 is located at the end of the creek with UTM-48 coordinates (701655, 2296119). According to the range of wind-wave, the wind, and hydrodynamic input data, the oil spill is expressed in three separate scenarios. A hypothetical oil spill can occur in each scenario with the wind direction, average wind velocity, and time period of 2015. The measure of these scenarios are explained as the following:

Scenario 1: oil spill occurred on May 13, 2015. The wind blew in a southeast direction with a constant value of 4.9 m/s. After 10 days, the volume of oil affected the Bach Dang River and Cua Cam River. An oil slick spread to the sea in the southeast direction and affected Cat Ba town. The oil spill polluted a coastal of over 10km (Figs. 8a, 8b).

Scenario 2: oil spill occurred on July 13, 2015. The wind blew in a southerly direction at a persistent value of 6.7 m/s. During 5 days, oil spread from southeast to south of Cat Ba coastal island and polluted this area. In 10 days, the oil spread to Tuan Chau and Dau Go Island in the north and Dau Be, But Day, Hang Trai and Bo Hoan Island in the south and southeast, respectively. The amount of oil spill primarily affected coastal areas along The creeks of Cat Ba Island were substantially influenced by the great deal of oil spill . Oil settled in this area, which was relatively large, and polluted the coastal islands (Figs. 8c, 8d).

Scenario 3: oil spill occurred on August 13, 2015. The wind blew in a south-westerly direction at a constant value of 5.4 m/s. After 10 days, oil slick spread with the rising tide throughout Dau Go and Tuan Chau Island and southeast of Cat Ba Island. The oil slick spread with the falling tide throughout Bau Be, But Day, Hang Trai Island and northeast of Cat Ba. The oil spread resulted in severe and the vicinity of its small islands (Figs. 8e, 8f).

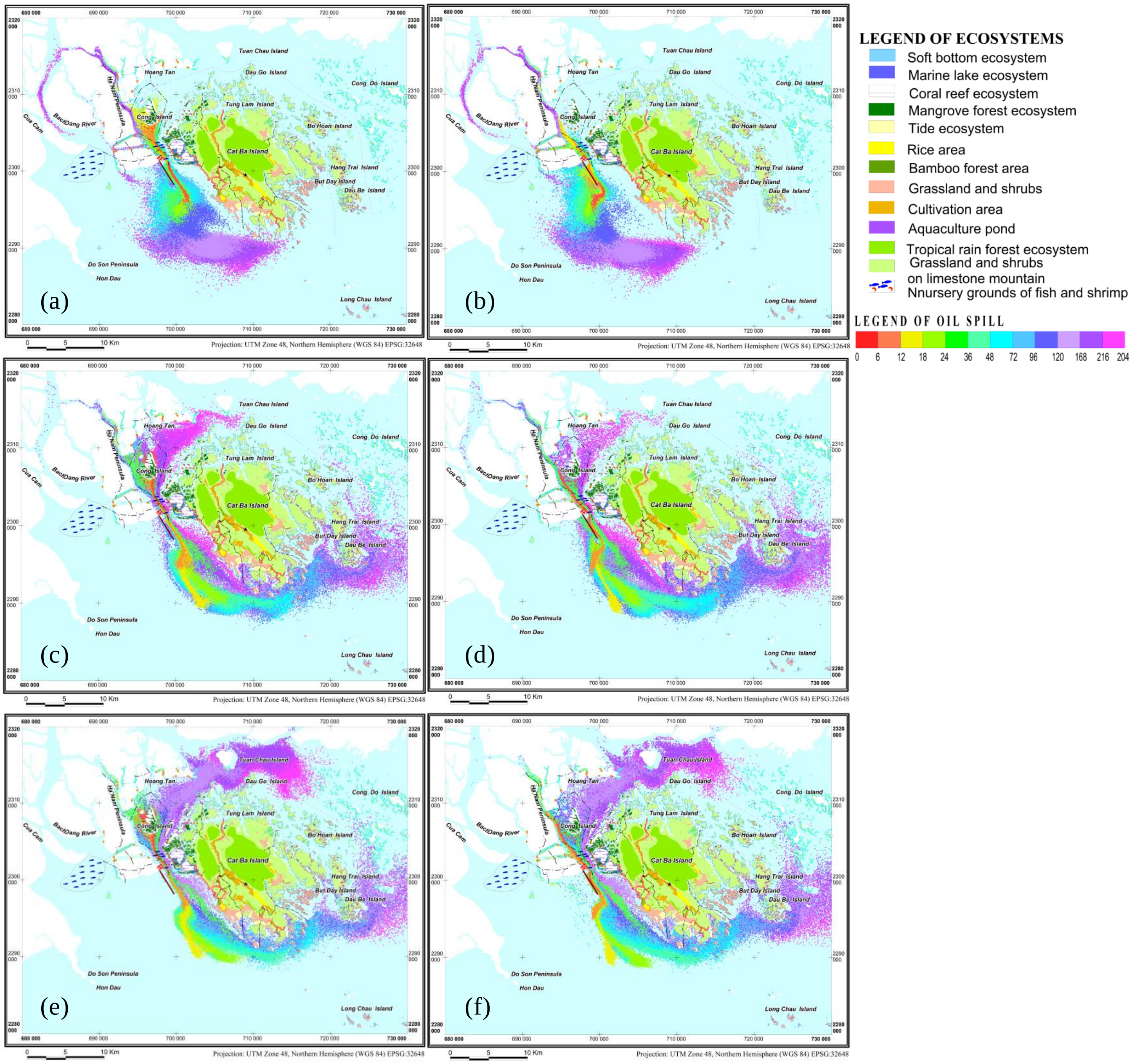

Figure 8 Results of oil spill pollution scenarios: Scenario 1 (a, b); Scenario 2 (c, d); Scenario 3: (e, f).

The results of the simulation with three scenarios combined with the ecosystem map of Cat Ba showed that oil spill occurred at Lach Huyen port affected a vast area. Oil spill impact assessment for Cat Ba ecosystem is presented in next section.

3.5. Oil spill impact assessment for Cat Ba ecosystem

According to the results of the analysis for three scenarios described in "Spill analysis model", the oil spill in two scenarios No. 1 at two positions SL1, SL2 do not affect Cat Ba Island. Scenario No. 2 and 3 significantly influenced Cat Ba Island, primarily the coastal shoreline in the northwest, southwest areas. Thus, we will establish the maps to impact assessment of oil slick to ecosystem biosphere reserve of Cat Ba Island following three scenarios (Fig. 8). According to the results of the analysis of the oil slick from the scenario No. 1 and the results of establishing map at SL1 and SL2 oil spill locations showed that oil slick does not put a worse effect on the ecosystem of Cat Ba Island. Oil slick only affects the fish and shrimp cultivation area at Cat Hai coastal and Cong Island. The oil slick affects the grasslands and shrubs in the south of Cat Ba town. However, the oil slick directly affects the mangrove forest on

Cong Island, which is far from Cat Ba Island (Figs. 8a, 8b).

The results of scenarios No. 2 and 3 showed that oil slick affects considerable proportion of Cat Ba Island, including the coast and small islands. An oil slick with a falling tide extends from the southwest to south of Cat Ba Island detrimental impacts on the coastal area. Figure 8c to figure 8f showed that oil slick caused the following pollution types in the southwest and southeast of Cat Ba Island: grassland and shrubs, rice area, and coral reef ecosystem. An oil slick with a rising tide extends from the northwest-north-northeast of Cat Ba causes pollution along the west coast through Dau Go Island. An oil slick causes pollution on mangrove forest ecosystem near Cong Island in the northwest of Cat Ba, nursery grounds for fish and shrimp in Cat Hai, aquaculture pond in the east of Cat Hai and marine lake ecosystem in the north of Cat Ba. The oil slick not only directly cause pollution on Cat Ba biosphere reserve ecosystems and surrounding areas but also affects on the tourism potential in the study site.

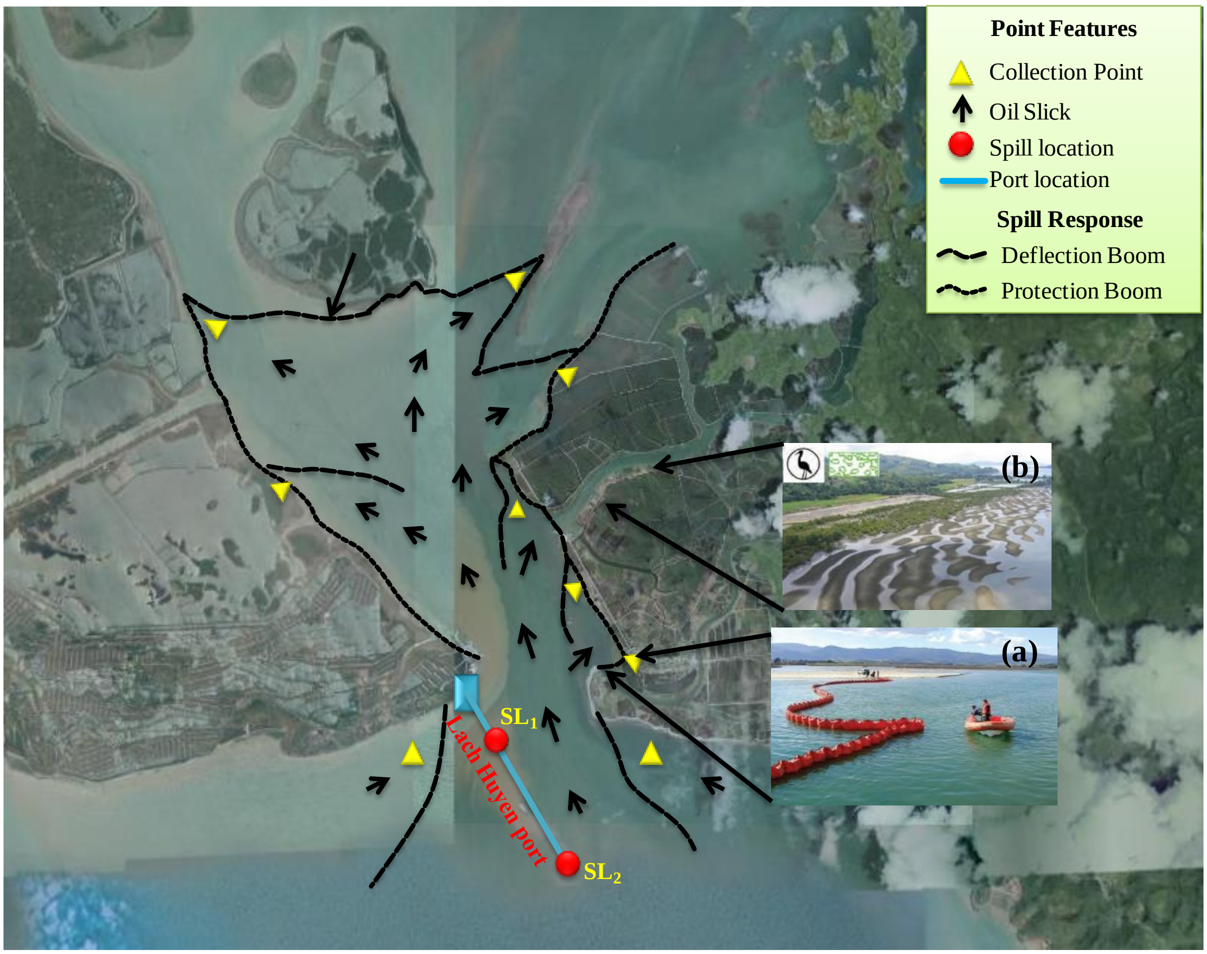

Figure 9 The tidal inlet protection strategy for Cat Ba Island: (a) Boom deployment site near the river mouth; (b) Tidal flat backed by mangroves and wetlands.

3.6. Oil Spill response

The objective of all oil spill response strategies should be to minimize the damage, both ecological and economic, that could be caused by an oil spill. The most obvious way to do this is to prevent the spilled oil from coming into contact with oil-sensitive resources. Most damage is done by spilled oil when it gets into shallow water or comes ashore. The objective of oil spill response actions at sea should be to prevent oil from reaching the shoreline or particularly sensitive resources at sea, such as fish spawning grounds (Lewis, 2001). The response actions can include: Using booms to contain the oil near the spill source; using sorbents to soak up the oil near the spill source; using booms and skimmers to contain and recover the oil at sea, before the oil drifts too close to the shore; using booms to protect a shoreline resource and divert the spilled oil away from it; using oil spill dispersants to disperse the oil into the water column before it approaches an oil-sensitive site. In this study, using floating boom is the best protection scenarios which can be collected the oil at the collection points (Fig. 9a). To establish effective protection strategies, the local and national experts need to analyze the hydrodynamic flow regime in the inlet areas, probable oil trajectories, habitat and human-use protection priorities. Thus, the deflection booms, the protection booms and the collection points will be arranged at the suitable positions to collect oil spills. The protection strategies have evaluated a height in this study when can be combined between a test of boom position, a suitable deflection angle, and an ability preventing oil spills. An example of the inlet protection strategies for Lach Huyen inlet is presented in Fig. 9. The tide inlet protection strategies are developed and tested before an oil spill occurs. This is a proactive planning rather than reactive with an oil spill response. Using the simulation results of "spill analysis model" will rapidly give the protection strategies to response with the oil spill-specific conditions, and ready calculated the length of the boom to protect the areas affected by an oil slick. Preparing and sharing of the protection strategies between the government and industry will be increasing the likelihood of successful deployment because everyone has agreed to the strategy and planning for its implementation.

4. CONCLUSION

In fact, the impact of oil spill on the environmental ecosystem is very serious. In this study, a two-dimensional hydrodynamic model was applied to simulate the spectral wind-wave, hydrodynamic flow regime, and the oil spill pollution. A GIS supportive software was applied to establish the ecosystem maps of Cat Ba Island. The calculation results from calibration and validation processes in the hydrodynamic model showed a high conformity between the calculated and observed water level data for the phase and water amplitude. The results from the wind-wave and hydrodynamic modules showed that the hydrodynamic regime is complicated in the nearshore areas. The simulation results from these spill scenarios showed that oil spills effect at Lach Huyen port areas and surrounding areas. The combination of the spill analysis results and the biological ecosystem maps of Cat Ba area provide an overview of oil spills. The hydrodynamic flow regime analysis and oil slick trajectories can give solutions to respond with oil slick by the application spill response plans. The response planning to oil spill incident was initially selected consistent with the natural conditions. If at the sensitive locations on the ocean, lakes and big rivers are prepared by response institutions with full equipment, it will be useful to implement and timely rescue. It means that we can control and significantly limit the damage from the other accidents. This response planning should be implemented and replicated in many other places.

CONFLICT OF INTEREST

The authors declare that there are no competing interests regarding the publication of this paper.

ACKNOWLEDGMENTS

We are thankful to Ton Duc Thang University, Vietnam, National Center Hydrometeorological Service and Institute of Marine Environment Resources for this research opportunity and for the facilities used to perform the study.

REFERENCE

1. Afandizadeh, S., Kalantari, N., Rezaeestakhruie, H., 2012. A partial linearization method for multi-objective continuous network design problem with environmental considerations. Int. J. Environ. Res. 6 (2), 381-390. DOI: 10.22059/IJER. 2012.505.
2. Ajibola, V.O, Ladipo, M.K., 2011. Sediment quality of effluent discharge channels from six industrial sites in Lagos, Nigeria. Int. J. Environ. Res. 5 (4), 901-908. DOI: 10.22059/ IJER.2011.447.
3. Akbar Mohammadi. 2017. Role of chemical reaction on concentrations of NO_2, NO, CO and O_3 in warm seasons - case study: Tehran city. *Climate Change*, 3(11), 832-841
4. Chao, X.B., Shankar, N.J., Wang, S., 2003. Development and application of oil spill model for Singapore coastal waters. J. Hydro. Eng. 129, 495-503. http://sci-hub.bz/10.1061/ (asce)0733-9429(2003)129:7(495).
5. Cho, Y.S., Kim, T.K., Jeong, W., Ha, T., 2012. Numerical simulation of oil spill in ocean. J App. Math. 2012, 15. DOI:10.1155/2012/681585.
6. Doan, Q.T., Nguyen, C.D., Chen, Y.C., Pawan, K.M., 2015. Application of environmental sensitivity index (ESI) maps of shoreline for the coastal oil spills: case study of Cat Ba Island, Vietnam. Environ. Earth Sci. 74 (04), 3433-3451. https://doi.org/10.1007/s12665-015-4380-0.
7. Doan, Q.T., Nguyen, C.D., Chen, Y.C., 2013. Trajectory modeling of marine oil spills: case study of Lach Huyen port, Vietnam. Low. Tech. Int. 15 (2), 41-51.
8. Doan, Q.T., Chen, Y.C., 2016. Application Environmental Sensitivity Index Maps for Coastal Oil Spill. LAP LAMBERT Academic Publishing, OmniScriptum GmbH & Co. KG, BahnhofstraBe 28, 66111 Saarbrücken Germany.
9. Daniel, P., Dandin, P., Josse, P., Skandraini, C., Benshila, R., Tiercelin, C., Cabioch, F., 2002. Towards better forecasting of oil slick movement at sea based on information from the Erika. In Proc. Third R&D Forum on High-Density Oil Spill Response, Brest, France: International Maritime

Organization.
10. http://www.meteorologie.eu.org/mothy/references/imo_erika.pdf
11. Deborah, P.F.M., Mark, A.J., Louis, C., 2001. Oil spill modeling for contingency planning and impact assessment and example application for Florida Power & Light. International Oil Spill Conference Proceedings: March 2001, 2001 (2), 873-881. https://doi.org/10.7901/2169-3358-2001-2-873.
12. FFI, 2003. Annual technical report: report on BP - Vietnam funding, Ha Long/Cat Ba conservation project and coastal biodiversity support project preparation phase, fauna and flora international (FFI), Hanoi, Vietnam.
13. https://www.systemdynamics.org/conferences/2010/proceed/papers/P1312.pdf
14. Gupta, H.V., Sorooshian, S., Yapo, P.O., 1999. Status of automatic calibration for hydrologic models: Comparison with multilevel expert calibration. J. Hydro. Eng. 4 (2), 135-143. https://doi.org/10.1061/(ASCE)1084-0699(1999)4: 2(135).
15. Ghasem Zolfaghari, Fatemeh Arab Amery, Mehri Delsouz. 2017. Investigating the status of air pollution and comparing the concentration of its major pollutants in Shiraz, Iran. *Climate Change*, 3(11), 810-815
16. Kavian, A., Fathollah Nejad, Y., Habibnejad, M., Soleimani, K., 2011. Modeling seasonal rainfall erosivity on a regional scale: A case study from northeastern Iran. Int. J. Environ. Res. 5 (4), 939-950. DOI: 10.22059/ijer.2011.451.
17. Komen, G.J., Cavaleri, L., Doneland, M., Hasselmann, K., Hasselmann, S., Janssen, P.A.E.M., 1994. Dynamics and modeling of ocean waves, Cambridge University Press, UK, 560. https://doi.org/10.1017/CBO9780511628955.
18. Lewis, A., 2001. Oil spill dispersants. SINTEF Report No, SFT 66FO1179. https://portal.helcom.fi/Archive/archive2/DISPERSANTS%20WS%202005_Presentation_Oil%20spill%20dispersant%20article%202001.pdf.
19. Mackay, D., Paterson, S., Trudel, K., 1980. A mathematical model of oil spill behavior. Environmental Protection Service, Fisheries and Environment Canada;
20. Nagheeby, M., Kolahdoozan, M., 2010. Numerical modeling of two-phase widow and oil slick transport in estuarine water. In. J. Environ. Sci. Tech. 7, 771-784. http://www.bioline.org.br/pdf?st10076.
21. Nash, J.E., Sutcliffe, J.V., 1970. River flow forecasting through conceptual models part I - A discussion of principles. J. Hydro. 10 (3), 282-290. https://doi.org/10.1016/0022-1694(70)90255-6.
22. Rahman, M.M., Al-Malack, M.H., 2012. Biochemical kinetics of cross flow membrane bioreactor processes in the treatment of refinery wastewater. Int. J. Environ. Res. 6 (1), 285-296. http://www.sid.ir/en/VEWSSID/J_pdf/108220120124.pdf.
23. Sekman, E., Top, S., Uslu, E., Varank, G., Bilgili, M.S., 2011. Treatment of oily wastewater from port waste reception facilities by electrocoagulation. Int. J. Environ. Res. 5 (4), 1079-1086. DOI: 10.22059/IJER.2011.466.
24. Sadatipour, S.M.T., Kiamehr, R., Abrehdary, M., Sharifi, A.R., 2012. The evaluation of sea surface topography models based on the combination of the satellite altimetry and the global Geoid Models in the Persian Gulf. Int. J. Environ. Res. 6 (3), 645-652. DOI: 10.22059/IJER.2012.534.
25. Soltani, N., Baftechi, L., Dezfulian, M., Shokravi, S., Alnajar, N., 2012. Molecular and morphological characterization of oil polluted microalgae. Int. J. Environ. Res. 6 (2), 481-492. https://ijer.ut.ac.ir/article_517_b20769e129fba99d46813f77e3007f06.pdf.
26. Quan, N.V., Thanh, T.D., Huy, D.V., 2010. Landscape and ecosystem of tropical limestone: Case study of the Cat Ba Islands, Vietnam. J. Ecology Environ. 33 (1), 23-36. http://dx.doi.org/10.5141/JEFB.2010.33.1.023
27. William, B.S., David, E.A., Rakesh, B., Christopher, Z., 2013. Development of a global oil spill modeling system. Earth Science Research 2. http://dx.doi.org/10.5539/esr.v2n2p52.
28. Yet, N.H., Ken, L.V., Ngai, N.D., 2007. Charging in species composition of reef coral building in Cat Ba Islands, Hai Phong. Proceeding Nat Symp on Basic Studies in Life SCI, 317-325.
29. Young, I.R., 1999. Wind-generated Ocean waves. Elsevier Ocean Engineering Book Series, Volume 2. (Eds) Bhattacharyya R and McCormick ME, Elsevier. https://www.elsevier.com/books/wind-generated-ocean-waves/young/978-0-08-043317-2.